Fluctuations of current-driven domain walls in the nonadiabatic regime

M. E. Lucassen* and R. A. Duine
Institute for Theoretical Physics, Utrecht University, Leuvenlaan 4, 3584 CE Utrecht, The Netherlands
(Received 23 April 2009; revised manuscript received 2 September 2009; published 22 October 2009)

We outline a general framework to determine the effect of nonequilibrium fluctuations on driven collective coordinates and apply it to a current-driven domain wall in a nanocontact. In this case the collective coordinates are the domain-wall position and its chirality that give rise to momentum transfer and spin transfer, respectively. We determine the current-induced fluctuations corresponding to these processes and show that at small frequencies they can be incorporated by two separate effective temperatures. As an application, the average time to depin the domain wall is calculated and found to be lowered by current-induced fluctuations. It is shown that current-induced fluctuations play an important role for narrow domain walls, especially at low temperatures.

DOI: 10.1103/PhysRevB.80.144421 PACS number(s): 72.25.Pn, 72.15.Gd, 72.70.+m, 75.60.−d

I. INTRODUCTION

Fluctuations play an important role in many areas of physics. The classic example is Brownian motion,[1] for example, of a colloidal particle in a suspension. The effect of collisions of the small particles, that constitute the suspension, with the colloid is modeled by stochastic forces. The strength of these forces is inferred from the famous fluctuation-dissipation theorem, which states that their variance is proportional to damping due to viscosity, and to temperature, and that their average is zero. If the suspension is driven out of equilibrium, the average force on the colloid will no longer be zero. Because of the nonequilibrium situation, the fluctuation-dissipation theorem, in principle, no longer holds, and the fluctuations cannot be determined from it anymore. Another explicit example of fluctuations in a driven system that do not obey the fluctuation-dissipation theorem is shot noise in the current in mesoscopic conductors, where the fluctuations are determined by the applied voltage instead of temperature. It is ultimately caused by the fact that the electric current is carried by discrete charge quanta, the electrons.[2]

The nonequilibrium system on which we focus in this paper is a current-driven domain wall[3,4] in a ferromagnetic conductor. Here the domain wall and the electrons play the role of the colloid and the suspension from the above example. There are two distinct processes that lead to current-induced domain-wall motion: spin transfer[5,6] and momentum transfer.[7] Physically, momentum transfer corresponds to the force exerted on the domain wall by electrons that are reflected by the domain wall or transmitted with different momentum. Spin transfer corresponds to electrons whose spin follows the magnetization of the domain wall adiabatically, thereby exerting a torque on the domain wall. Most experiments[8–12] are in the adiabatic regime, where the electron spin follows the direction of magnetization adiabatically and where the spin-transfer torque is the dominant effect. The effect of spin relaxation on spin transfer in the adiabatic limit, leading to a dissipative spin-transfer torque, was discussed theoretically[13] and experimentally.[14,15] The experiments by Feigenson *et al.*[16] with $SrRuO_3$ films, on the other hand, are believed to be in the nonadiabatic limit where domain walls are narrow compared to the Fermi wavelength and momentum transfer is dominant. In this paper, we will mostly consider narrow domain walls in nanocontacts.[17–19]

Apart from the forces and torques on the magnetization texture due to nonzero average current, there are also current-induced fluctuations on the magnetization[20,21] that ultimately have their origin in shot noise in the spin and charge current. Foros *et al.*[20] studied the effects of spin-current shot noise in single-domain ferromagnets and found that for large voltage and low temperature the fluctuations are determined by the voltage and not by the temperature. Chudnovskiy *et al.*[22] study spin-torque shot noise in magnetic tunnel junctions and in Ref. 23 Foros *et al.* consider a general magnetization texture and work out the current-induced magnetization noise and inhomogeneous damping in the adiabatic limit. Basko and Vasilov[24] have studied nonequilibrium stochastic dynamics of a single-domain magnetic particle taking into account fluctuations in the magnitude of the magnetization.

In this paper, we determine the effect of current-induced fluctuations on a domain wall in the nonadiabatic limit. We show that it leads to anisotropic damping and fluctuations and show that the fluctuations can be described by two separate voltage-dependent effective temperatures corresponding to momentum transfer and spin transfer. We show that these effective temperatures differ considerably from the actual temperature for parameter values used in experiments with nanocontacts. From our model, we also determine the momentum transfer and the adiabatic spin-transfer torque on the driven domain wall, as well as the damping corresponding to these processes.

II. MODEL

In this section, we present a model for treating a domain wall out of equilibrium. We develop a variational principle within the Keldysh formalism and then work out the various Green's functions within Landauer-Büttiker transport theory.

A. Keldysh theory

We consider a one-dimensional model of spins coupled to conduction electrons. The action is on the Keldysh contour C given by

$$S[\mathbf{\Omega},\psi,\psi^*] = \int_C dt \Bigg\{ -E_{\mathrm{MM}}[\mathbf{\Omega}] + \int \frac{dx}{a} \Bigg\{ -\hbar \mathbf{A}[\mathbf{\Omega}(x,t)] \cdot \frac{\partial \mathbf{\Omega}(x,t)}{\partial t} + \frac{\Delta}{2} \sum_{\sigma,\sigma'} \psi^*_\sigma(x,t) \mathbf{\Omega}(x,t) \cdot \boldsymbol{\tau}_{\sigma,\sigma'} \psi_{\sigma'}(x,t) + \sum_\sigma \psi^*_\sigma(x,t) \left[i\hbar \frac{\partial}{\partial t} + \frac{\hbar^2 \nabla^2}{2m} - V(x) \right] \psi_\sigma(x,t) \Bigg\} \Bigg\}, \tag{1}$$

where a is the lattice spacing, $\mathbf{A}(\mathbf{\Omega})$ is the fictitious vector potential that obeys $\nabla_{\mathbf{\Omega}} \times \mathbf{A}(\mathbf{\Omega}) = \mathbf{\Omega}$ and ensures precessional motion of $\mathbf{\Omega}$, Δ is the exchange-splitting energy, $\mathbf{\Omega}(x,t)$ is a unit vector in the direction of the magnetization, $\boldsymbol{\tau}$ is the vector of Pauli matrices, and $V(x)$ is an arbitrary scalar potential. The fields $\psi^*_\sigma, \psi_\sigma$ represent the conduction electrons with spin projection $\sigma \in \{\uparrow, \downarrow\}$. The micromagnetic energy functional $E_{\mathrm{MM}}[\mathbf{\Omega}]$ is given by

$$E_{\mathrm{MM}}[\mathbf{\Omega}] = -\int \frac{dx}{a} [J \mathbf{\Omega}(x,t) \cdot \vec{\nabla}^2 \mathbf{\Omega}(x,t) - K_\perp \Omega_y^2(x,t) + K_z \Omega_z^2(x,t)], \tag{2}$$

with $J>0$ the spin stiffness and $K_\perp > 0$ and $K_z > 0$ the hard-axis and easy-axis anisotropy constants, respectively. The micromagnetic energy functional in Eq. (2) has stationary domain-wall solutions $\mathbf{\Omega}(x) = (\sin\theta_{\mathrm{dw}} \cos\phi_{\mathrm{dw}}, \sin\theta_{\mathrm{dw}} \sin\phi_{\mathrm{dw}}, \cos\theta_{\mathrm{dw}})$.[7] These stationary solutions are the basis for a time-dependent variational *ansatz* given by

$$\theta_{\mathrm{dw}} = 2 \arctan\{e^{[x-X(t)]/\lambda}\}; \quad \phi_{\mathrm{dw}} = \phi(t), \tag{3}$$

where $\lambda = \sqrt{J/K_z}$ is the domain-wall width. In the above, we have taken the domain-wall position $X(t)$ to be time dependent. Furthermore, $\phi(t)$ is the angle of the magnetization at the center with the easy plane, the so-called chirality. Using the above ansatz, the first two terms in the action in Eq. (1) simplify to

$$S_0[X,\phi] = \hbar N \int_C dt \left[\frac{\dot{X}}{\lambda} \phi - \frac{K_\perp}{2} \sin 2\phi \right]. \tag{4}$$

Here, $N = 2\lambda/a$ is the number of spins in the domain wall. Note that in three dimensions, the number of spins increases by a factor A/a^2, where A is the cross-sectional area of the sample.

Stochastic forces are not obtained in a natural way by variation in the real-time action or the Euclidean action in the system. The functional Keldysh formalism,[25] however, provides us with the (current-induced and thermal) noise terms automatically, and is therefore more useful for our purposes. By expanding in collective coordinates X and ϕ

$$\mathbf{\Omega} = \mathbf{\Omega}|_0 + X \frac{\partial \mathbf{\Omega}}{\partial X}\bigg|_0 + \phi \frac{\partial \mathbf{\Omega}}{\partial \phi}\bigg|_0 + \mathrm{h.o.}, \tag{5}$$

where from here onward the subscript $|_0$ denotes evaluation at $X=\phi=0$, we derive an effective action on the Keldysh contour for the collective coordinates. In order to find an effective action up to terms quadratic in coordinates X and ϕ, it turns out to be sufficient to expand Eq. (5) up to linear order in these coordinates. The majority of second-order terms in Eq. (5) cancel out on the Keldysh contour and the terms that remain are merely an artefact of the approximation that would not arise when treating the full problem. They should therefore not be taken into account.

The total action is now given by $S[X,\phi,\psi^*,\psi] = S_0[X,\phi] + S_{\mathrm{C}}[X,\phi,\psi^*,\psi] + S_{\mathrm{E}}[\psi^*,\psi]$. The contribution to the action in Eq. (1) that describes coupling between magnetization and electrons is given by

$$S_{\mathrm{C}}[X,\phi]|_0 = \frac{\Delta}{2} \int_C dt \int dx \sum_{\sigma,\sigma'} \psi^*_\sigma(x,t) \times [(\partial_X \mathbf{\Omega} \cdot \boldsymbol{\tau})|_0 X(t) + (\partial_\phi \mathbf{\Omega} \cdot \boldsymbol{\tau})|_0 \phi(t)] \psi_{\sigma'}(x,t). \tag{6}$$

The electron action reads

$$S_{\mathrm{E}}[\psi^*,\psi] = \int_C dt \int dx \sum_{\sigma,\sigma'} \psi^*_\sigma(x,t) \times \left\{ \left[i\hbar \frac{\partial}{\partial t} + \frac{\hbar^2 \nabla^2}{2m} - V(x) \right] \delta_{\sigma\sigma'} - V_{\sigma\sigma'}(x) \right\} \times \psi_{\sigma'}(x,t), \tag{7}$$

with the potential $V_{\sigma\sigma'}$, which arises from the zeroth-order term $\mathbf{\Omega}|_0$, given by

$$V_{\sigma\sigma'}(x) = -\frac{\Delta}{2} \begin{pmatrix} \cos\theta_{\mathrm{dw}} & \sin\theta_{\mathrm{dw}} \\ \sin\theta_{\mathrm{dw}} & -\cos\theta_{\mathrm{dw}} \end{pmatrix}\bigg|_0. \tag{8}$$

At this point, we could integrate out the fermions exactly since the action is quadratic in the fermions. However, since we are only interested in the perturbations up to second order, we choose to do perturbation theory in X and ϕ, which enables us to derive an effective action on the Keldysh contour for these coordinates

$$S_{\mathrm{eff}}[X,\phi] \simeq S_0[X,\phi] + \langle S_{\mathrm{C}}[X,\phi,\psi^*,\psi] \rangle + \frac{i}{2\hbar} (\langle S^2_{\mathrm{C}}[X,\phi,\psi^*,\psi] \rangle - \langle S_{\mathrm{C}}[X,\phi,\psi^*,\psi] \rangle^2). \tag{9}$$

Here, the expectation values are taken with respect to the electron action $S_{\mathrm{E}}[\psi^*,\psi]$ in Eq. (7), i.e.,

$$\langle O[X,\phi,\psi^*,\psi] \rangle = \int d[\psi^*] d[\psi] e^{iS_{\mathrm{E}}[\psi^*,\psi]/\hbar} O[X,\phi,\psi^*,\psi]. \tag{10}$$

In the next section, we evaluate these expectation values in more detail.

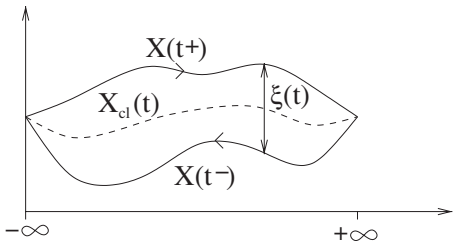

FIG. 1. A path that the coordinate X might take on the Keldysh contour. The deviation from the (classical) mean path is denoted by $\xi(t)$.

Since we now have an effective action as a function of the collective coordinates X and ϕ, we can make use of the advantages of the Keldysh formalism. The effective action in Eq. (9) is integrated from $t=-\infty$ to $t=\infty$ and back.

The forward and backward paths are different, as is shown for the coordinate X in Fig. 1, such that we write

$$X(t^{\pm}) = X_{\rm cl}(t) \pm \frac{\xi(t)}{2}; \quad \phi(t^{\pm}) = \phi_{\rm cl}(t) \pm \frac{\kappa(t)}{2};$$

$$\int_C dt f(t) = \int_{-\infty}^{\infty} dt^{+} f(t^{+}) + \int_{\infty}^{-\infty} dt^{-} f(t^{-}), \tag{11}$$

with the assumption that the variations ξ and κ are small. Furthermore, they obey the boundary conditions $\xi(\pm\infty)=\kappa(\pm\infty)=0$. Integrating the effective action over this contour and using the method outlined in Refs. 21 and 25, we ultimately obtain the Langevin equations for a domain wall

$$\frac{\dot{X}_{\rm cl}(t)}{\lambda} - \alpha_{\phi}\dot{\phi}_{\rm cl}(t) = K_{\perp}\cos 2\phi_{\rm cl}(t) + F_{\phi} + \eta_{\phi}(t), \tag{12}$$

$$\dot{\phi}_{\rm cl}(t) + \alpha_{X}\frac{\dot{X}_{\rm cl}(t)}{\lambda} = -F_{X} + \eta_{X}(t). \tag{13}$$

The calculations that lead to these equations of motion are outlined in the Appendix. The stochastic contributions η_{ϕ} and η_{X} in this expression arise via a Hubbard-Stratonovich transformation of terms quadratic in ξ and κ.

The expectation value of the action $S_{\rm C}[X,\phi,\psi^{*},\psi]$ in the effective action in Eq. (9) provides us with the forces

$$F_i = \frac{\Delta}{\hbar N}\sum_{\nu,\sigma,\sigma'} G^{<}_{\nu,\sigma,\sigma'}(0)\langle\nu,\sigma|\partial_i\mathbf{\Omega}|_0\cdot\boldsymbol{\tau}|\nu,\sigma'\rangle, \tag{14}$$

where the index $i\in\{X/\lambda,\phi\}$. Note that in this expression, F_{ϕ} corresponds to spin transfer and F_X to momentum transfer. As we will see later on, $\partial_{\phi}\mathbf{\Omega}|_0\cdot\boldsymbol{\tau}$ is associated with the divergence of the spin current and $\partial_X\mathbf{\Omega}|_0\cdot\boldsymbol{\tau}$ is associated with the force of the domain wall on the conduction electrons. The latter is, in the absence of disorder, proportional to the resistance of the domain wall.[7] The lesser Green's function in this expression is defined by $G_{\nu,\sigma,\sigma'}(t,t') = \theta(t,t')G^{>}_{\nu,\sigma,\sigma'}(t-t') + \theta(t',t)G^{<}_{\nu,\sigma,\sigma'}(t-t')$, where the Heaviside step functions are defined on the Keldysh contour. Note that the lesser Green's function in Eq. (14) is evaluated at equal times $t=t'$. Furthermore, we have expanded the Keldysh Green's function according to $iG_{\sigma,\sigma'}(x,t;x',t') \equiv \langle\psi_{\sigma}(x,t)\psi^{*}_{\sigma'}(x',t')\rangle = i\Sigma_{\nu}G_{\nu,\sigma,\sigma'}(t,t')\chi_{\nu,\sigma}(x)\chi^{*}_{\nu,\sigma'}(x')$, where χ and χ^{*} are electron eigenstates in the presence of a static domain wall that are labeled by ν. In terms of these states, the matrix elements are defined as

$$\int dx\langle\nu,\sigma|\hat{O}|\nu',\sigma'\rangle = \int dx\chi_{\nu,\sigma}(x)\hat{O}_{\sigma,\sigma'}(x)\chi^{*}_{\nu',\sigma'}(x). \tag{15}$$

The damping terms in Eqs. (12) and (13) follow from the second-order terms in the perturbation theory in X and ϕ and read $\alpha_i = \mp\,{\rm Im}[\tilde{\Pi}^{(\pm)}_i(\omega)]/(N\hbar\omega)$ for $\omega\to 0$ with $\tilde{\Pi}^{(\pm)}(\omega)$ the response function given below. We consider the low-frequency limit of the various response functions, which is a good approximation because the motion of the collective coordinates is on a much slower time scale than the electronic system. Since the action in Eq. (1) is quadratic in the electron fields, we use Wick's theorem to write the response function in terms of electron Green's functions

$$\begin{aligned}\tilde{\Pi}^{(\pm)}_i(\omega) = \mp\frac{\Delta^2}{4\hbar}\sum_{\nu,\nu'}\sum_{\sigma,\sigma'}\sum_{\rho,\rho'}&[G^{>}_{\nu,\sigma,\rho'}(\omega)G^{<}_{\nu',\rho,\sigma'}(-\omega)\\ &- G^{<}_{\nu,\sigma,\rho'}(\omega)G^{>}_{\nu',\rho,\sigma'}(-\omega)]\langle\nu,\sigma|\partial_i\mathbf{\Omega}|_0\cdot\boldsymbol{\tau}|\nu',\sigma'\rangle\\ &\times\langle\nu',\rho|\partial_i\mathbf{\Omega}|_0\cdot\boldsymbol{\tau}|\nu,\rho'\rangle.\end{aligned} \tag{16}$$

The functions $G^{>}(\pm\omega)$ and $G^{<}(\pm\omega)$ denote Fourier transforms of $G^{>}[\pm(t-t')]$ and $G^{<}[\pm(t-t')]$, respectively.

Without needing to assume (approximate) equilibrium, the Keldysh formalism provides us with an expression for the strength of the fluctuations in both coordinates $\langle\eta_i(t)\eta_j(t')\rangle = i\delta_{i,j}\Pi^{\rm K}_i(t-t')/(\hbar N^2) \simeq i\delta_{i,j}\tilde{\Pi}^{\rm K}_i(\omega=0)\delta(t-t')/(\hbar N^2)$ and $\langle\eta_i(t)\rangle=0$. The Keldysh component of the response function contains similar matrix elements as the damping terms and is given by

$$\begin{aligned}\tilde{\Pi}^{\rm K}_i(\omega) = \frac{\Delta^2}{2\hbar}\sum_{\nu,\nu'}\sum_{\sigma,\sigma'}\sum_{\rho,\rho'}&\times[G^{>}_{\nu,\sigma,\rho'}(\omega)G^{<}_{\nu',\rho,\sigma'}(-\omega)\\ &+ G^{<}_{\nu,\sigma,\rho'}(\omega)G^{>}_{\nu',\rho,\sigma'}(-\omega)]\times\langle\nu,\sigma|\partial_i\mathbf{\Omega}|_0\cdot\boldsymbol{\tau}|\nu',\sigma'\rangle\\ &\times\langle\nu',\rho|\partial_i\mathbf{\Omega}|_0\cdot\boldsymbol{\tau}|\nu,\rho'\rangle.\end{aligned} \tag{17}$$

We now define two separate effective temperatures

$$k_{\rm B}T_{{\rm eff},i} \equiv \frac{i\tilde{\Pi}^{\rm K}_i(\omega=0)}{2\alpha_i N^2}. \tag{18}$$

These effective temperatures are defined such that Eqs. (12) and (13) obey the fluctuation-dissipation theorem with the effective temperatures. In the absence of a bias voltage, the effective temperatures reduce to the actual temperature divided by the number of spins in the system. That the effective temperatures are proportional to $1/N$ is understood because they describe fluctuations in collective coordinates made up of N degrees of freedom.[26] We note that our for-

malism applies to any set of collective coordinates and is not necessarily restricted to the example of a domain wall. We also point out that going beyond the low-frequency limit and taking into account the full frequency dependence in Eq. (17) leads to colored noise. In this case, effective temperatures may no longer be unambiguously defined.[27]

B. Landauer-Büttiker transport

We now evaluate Eqs. (14)–(17) using the Landauer-Büttiker formalism, i.e., the scattering theory of electronic transport. In order for this formalism to apply, the phase-coherence length L_ϕ must be larger than the domain-wall width λ. To compute the terms in the Langevin Eqs. (12) and (13) explicitly, we need to find the matrix elements $\langle \nu,\sigma|\partial_i \mathbf{\Omega}|_0 \cdot \boldsymbol{\tau}|\nu',\sigma'\rangle$ and the Green's functions. The Keldysh Green's function is in terms of scattering states $\chi_\sigma^{\zeta\kappa\varepsilon}(x)$ given by

$$iG_{\sigma,\sigma'}(x,t;x',t') = \int_0^\infty \frac{d\varepsilon}{2\pi}\sum_{\zeta,\kappa}\frac{2m/\hbar^2}{k_{\zeta\kappa}} e^{-i/\hbar\varepsilon(t-t')}\chi_{\sigma'}^{\zeta\kappa\varepsilon}(x) \times[\chi_\sigma^{\zeta\kappa\varepsilon}(x')]^* \times \{\theta(t,t')[1-N_F(\varepsilon-\mu_\zeta)] - \theta(t',t)N_F(\varepsilon-\mu_\zeta)\}, \tag{19}$$

with μ_ζ the chemical potential of the lead on side $\zeta \in \{\mathrm{L(left)},\mathrm{R(right)}\}$, $\kappa \in \{\uparrow,\downarrow\}$ the spin of the incoming particles and $N_F(x)$ the Fermi distribution function. We choose $V(x)=0$ for convenience. The momenta $k_{\zeta\kappa}$ associated with an energy ε are given by $k_{L\uparrow}=k_{R\downarrow}=k_F\sqrt{(\varepsilon+\Delta/2)/\varepsilon_F}$ and $k_{R\uparrow}=k_{L\downarrow}=k_F\sqrt{(\varepsilon-\Delta/2)/\varepsilon_F}$, where $k_F=\sqrt{2m\varepsilon_F/\hbar^2}$, with ε_F the Fermi energy in the leads. The index ν used earlier now contains information on the origin, spin, and energy of the incoming particle. Note that evaluating the various expectation values using Eq. (19) implies that we are doing perturbation theory around a static domain wall in the presence of a steady-state transport current. In particular, there is no backaction of the domain-wall dynamics on the current. This approach makes a description using effective temperatures possible. We define the asymptotic expression for the scattering states in terms of transmission and reflection coefficients,

$$\chi_\sigma^{L\kappa\varepsilon} = \begin{cases} \delta_{\sigma,\kappa}e^{ik_{L\kappa}x} + \delta_{\sigma,\gamma}\sqrt{\dfrac{k_{L\kappa}}{k_{L\gamma}}}r_{\gamma\kappa}(\varepsilon)e^{-ik_{L\gamma}x}, & x\to-\infty; \\ \delta_{\sigma,\gamma}\sqrt{\dfrac{k_{L\kappa}}{k_{R\gamma}}}t_{\gamma\kappa}(\varepsilon)e^{ik_{R\gamma}x}, & x\to+\infty, \end{cases} \tag{20}$$

where summation over spin-index $\gamma \in \{\uparrow,\downarrow\}$ is implied and with a similar expression for right-incoming particles. These scattering states are illustrated in Fig. 2. From the explicit form of the ansatz, it is easily seen that $\partial\mathbf{\Omega}/\partial X=-\partial\mathbf{\Omega}/\partial x$ which enables us to write $(\Delta/2)(\partial\mathbf{\Omega}/\partial X)|_0\cdot\tau_{\sigma,\sigma'} = \partial_x V_{\sigma,\sigma'}(x)$. Here ∂_x denotes a derivative with respect to x and $V_{\sigma,\sigma'}(x)$ is the potential given in Eq. (8). Furthermore, one can check that $(\partial\mathbf{\Omega}/\partial\phi)\cdot\boldsymbol{\tau}_{\sigma\sigma'}|_0=-(\boldsymbol{\tau}_{\sigma\sigma'}\times\mathbf{\Omega})|_0^z$, where uppercase z denotes the z component of this cross product. The expectation value of this quantity is directly related to

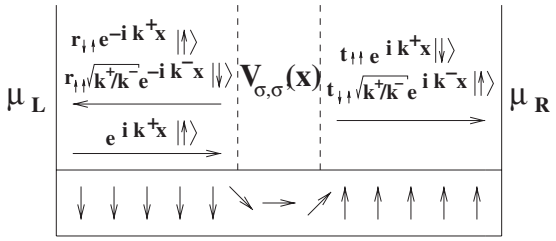

FIG. 2. The asymptotic form of the scattering state for a particle incoming from the left reservoir with spin up, i.e., the state $\chi_\sigma^{L\uparrow\varepsilon}$. We denoted $k^\pm=k_F\sqrt{(\varepsilon\pm\Delta/2)/\varepsilon_F}$, μ_L and μ_R are the chemical potentials in the left and right reservoir, respectively. The arrows on the bottom indicate the magnetization direction, the electrons experience a potential at the position of the domain wall.

the divergence of the spin current J_s^z, which measures the z component of the total spin current

$$\partial_x J_s^z(x) = \frac{\Delta}{2}\sum_{\sigma,\sigma'}\chi_\sigma^*(x)[\boldsymbol{\tau}_{\sigma\sigma'}\times\mathbf{\Omega}(x)]_0^z\chi_{\sigma'}(x). \tag{21}$$

In this expression, χ is a solution to the time-independent Schrödinger equation with the potential $V_{\sigma,\sigma'}(x)$. The spin current is defined as

$$J_s^z(x) = \frac{\hbar^2}{4mi}\sum_{\sigma,\sigma'}\{\chi_\sigma^*(x)\tau_{\sigma\sigma'}^z[\partial_x\chi_{\sigma'}(x)] - [\partial_x\chi_\sigma^*(x)]\tau_{\sigma\sigma'}^z\chi_{\sigma'}(x)\}. \tag{22}$$

From this, we observe that F_ϕ determined by Eq. (14) is indeed proportional to the divergence of spin current and hence corresponds to spin transfer.

We define $\mu_L=\mu+|e|V$ and $\mu_R=\mu\simeq\varepsilon_F$. The expressions for the Green's function and the scattering states in Eqs. (19) and (20) now allow us to write Eqs. (14)–(18) in terms of transmission and reflection coefficients, the applied voltage V, and $k_F\lambda$. For example, the momentum transfer in Eq. (14), with $i=X$, is up to first order in $|e|V/\varepsilon_F$ given by

$$F_X \simeq \frac{|e|V}{2\pi\hbar N}k_F\lambda\left[\sqrt{\frac{\varepsilon+\Delta/2}{\varepsilon_F}}(1+R_{\uparrow\uparrow}-T_{\downarrow\downarrow}+R_{\uparrow\downarrow}-T_{\downarrow\uparrow}) + \sqrt{\frac{\varepsilon-\Delta/2}{\varepsilon_F}}(1+R_{\downarrow\downarrow}-T_{\uparrow\uparrow}+R_{\downarrow\uparrow}-T_{\uparrow\downarrow})\right], \tag{23}$$

Here, the reflection and transmission coefficients are defined as $R_{\sigma\sigma'}=R_{\sigma\sigma'}(\varepsilon=\varepsilon_F)$ with $R_{\sigma\sigma'}(\varepsilon)\equiv|r_{\sigma\sigma'}(\varepsilon)|^2$ and equivalently for the transmission coefficients. Note that, although the coefficients are evaluated at the Fermi energy, they also depend on the ratio Δ/ε_F. The expression for the momentum transfer in Eq. (23) clearly demonstrates its correspondence to electrons scattering off the domain wall: it increases for increasing reflection and decreases for increasing transmission. The explicit form of the spin-transfer torque F_ϕ has $\propto T_{\downarrow\uparrow}$ as leading term, corresponding to electrons that follow the domain-wall magnetization adiabatically.

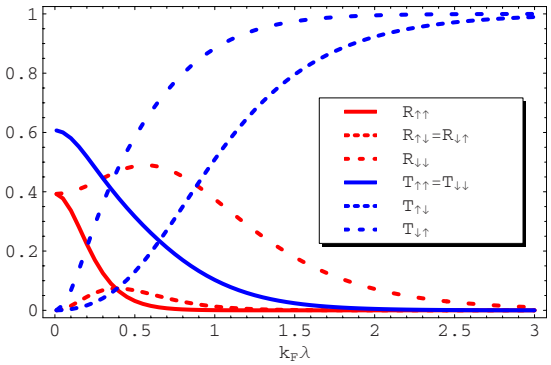

FIG. 3. (Color online) Transmission and reflection coefficients as functions of $k_F\lambda$ for $\Delta/2\varepsilon_F=0.8$ and $V=0$.

The reflection and transmission coefficients are obtained by solving the Schrödinger equation of the system numerically and matching the results to the asymptotic behavior in Eq. (20). As an example, we present the coefficients for $\Delta/2\varepsilon_F=0.8$ as a function of $k_F\lambda$ in Fig. 3.

III. RESULTS

As we have shown in the previous section, we are able to express Eqs. (14)–(17) in terms of transmission and reflection coefficients using Landauer-Büttiker transport, like in Eq. (23). As indicated, these coefficients are obtained by numerically solving the Schrödinger equation.

In the limit of small voltage, Eq. (23) is the exact expression for the momentum transfer. In fact, the momentum transfer as well as the spin-transfer torque are for small $|e|V/\varepsilon_F$ proportional to the voltage, in agreement with the fact that these quantities are usually described as linear with the spin current.[7] We present the ratio of these forces that measures the degree of nonadiabaticity, denoted by $F_X/F_\phi=\beta$, as a function of $k_F\lambda$ for several values $\Delta/2\varepsilon_F$ in Fig. 4.

In Fig. 4, the dashed curves show the result obtained directly from Eq. (23) and the expression for F_ϕ. We see that β is large for small $k_F\lambda$. Small $k_F\lambda$ implies narrow domain walls and therefore a large gradient in the magnetization.

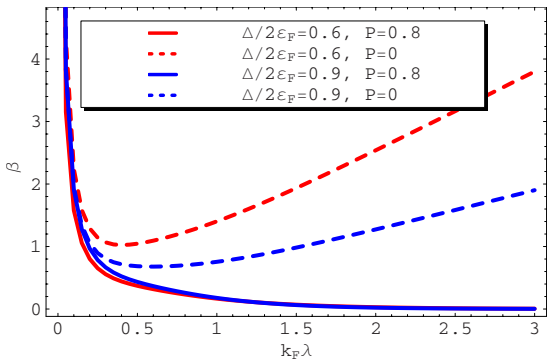

FIG. 4. (Color online) The parameter $\beta=F_X/F_\phi$ as a function of $k_F\lambda$ for $\Delta/2\varepsilon_F=0.6$ and $\Delta/2\varepsilon_F=0.9$, both at zero voltage. The dashed curves are obtained for $P=0$, the solid lines are obtained for a polarization of $P=0.8$.

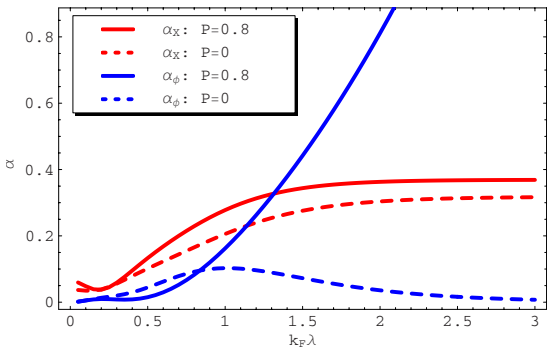

FIG. 5. (Color online) The damping parameters α_X and α_ϕ as a function of $k_F\lambda$ for $\Delta/2\varepsilon_F=0.9$, both at zero voltage. The dashed curves are obtained for $P=0$, the solid lines are obtained for a polarization of $P=0.8$.

This translates to a high potential and therefore large reflection coefficients. The ratio, however, does not vanish for large $k_F\lambda$, which one would expect since this is the adiabatic limit but instead acquires a linear dependence on $k_F\lambda$. Mathematically, this is caused not by an increase in momentum transfer but instead by a vanishing spin transfer. We can make sure that the spin transfer does not vanish by taking into account the polarization of the incoming electron current.[28,29] If we do take this into account, such that $R_{\sigma\uparrow}\to R_{\sigma\uparrow}(1+P)$, $R_{\sigma\downarrow}\to R_{\sigma\downarrow}(1-P)$, and equivalently for transmission coefficients, we find for $P=0.8$ the solid curves in Fig. 4. We see that these curves indeed go to zero in the adiabatic limit $k_F\lambda\gg 1$. From Fig. 4, it is clear that the polarization plays a big role from values $k_F\lambda\simeq 0.3$ onwards. Note that our theory does not take into account the dissipative spin-transfer torque, which gives similar contributions as momentum transfer.[13]

For the damping parameters α_X and α_ϕ, we find that for small $|e|V/\varepsilon_F$, they both acquire corrections linear in the voltage, in agreement with Katsura *et al.*[30] and Núñez and Duine.[21] The dependence on $k_F\lambda$ is much less trivial, as is shown in Fig. 5, where the curves are taken at zero voltage.

The unpredictable behavior of the damping parameters as a function of $k_F\lambda$ for small $k_F\lambda$ arises from the details of the solutions of the Schrödinger equation. For large $k_F\lambda$, we see that without polarization α_ϕ goes to zero, whereas for nonzero polarization, it increases quadratically. This is understood from the fact that damping in the angle ϕ arises from emission of spin current. This in its turn is closely related to spin-transfer torque, which goes to zero for $P=0$ but assumes nonzero values for $P>0$, as was discussed earlier in this section. It should be noted, however, that this approach breaks down for large values $k_F\lambda$ since we then lose phase coherence as $\lambda>L_\phi$. Furthermore, the polarization could be addressed in a more rigorous way by taking into account more transverse channels. Note that the fact that $\alpha_X\neq\alpha_\phi$ is a specific example of inhomogeneous damping as discussed by Foros *et al.*[23]

The effective temperatures of the system depend on the dimensionless parameters $k_F\lambda$ and $\Delta/2\varepsilon_F$. In Fig. 6 we plot the effective temperatures for X and ϕ as functions of $|e|V/k_BT$ for $k_F\lambda=1$ and several values $\Delta/2\varepsilon_F$. The solid curves are obtained for $P=0.6$, the dashed curves do not take

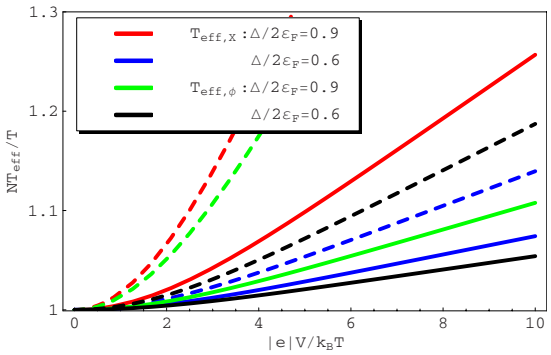

FIG. 6. (Color online) The effective temperatures $NT_{\mathrm{eff},X}/T$ and $NT_{\mathrm{eff},\phi}/T$ as a function of $|e|V/k_BT$ for $\Delta/2\varepsilon_F=0.6$ or $\Delta/2\varepsilon_F=0.9$, all at $k_F\lambda=1$. The dashed curves are for $P=0$, the solid curves are for $P=0.6$.

into account polarization. Note that the effective temperatures due to current-induced fluctuations can be substantially larger than the actual temperature and are for large voltage proportional to $|e|V$. This is modeled by introducing an effective temperature.

As an application of the effective temperatures derived above, we compute depinning times as a function of the voltage. We expect the increase in the effective temperature, i.e. an increase in the fluctuations, to translate into a decrease in the depinning times. The effective temperature $T_{\mathrm{eff},X}$, for example, influences depinning from a spatial potential for the domain wall, such as a nanoconstriction. We model the pinning potential by a potential well of width 2ξ, given by $V=\Delta V(X^2/\xi^2-1)\theta(|X|-\xi)$.[7] Using Arrhenius' law, the escape time is given by $\log(\tau\nu_0)=N(\Delta V-\hbar F_X\xi/\lambda)/k_BT_{\mathrm{eff},X}$, where $\nu_0\sim\Delta V/\hbar$ is the attempt frequency. Note that the effect of the momentum transfer is determined by the ratio $\xi/\Delta V$ and that the force itself is still dependent on the number of spins N. We show our results for $\Delta V\lambda/\xi=1$ meV, $N=10$ and several temperatures in Fig. 7. The results for $T_{\mathrm{eff}}=T$ are also shown. Note that current-induced fluctuations indeed decrease depinning times with respect to the result with the actual temperature. Here, we did not take into account polarization, as we have seen that this does not change the results significantly for small $k_F\lambda$.

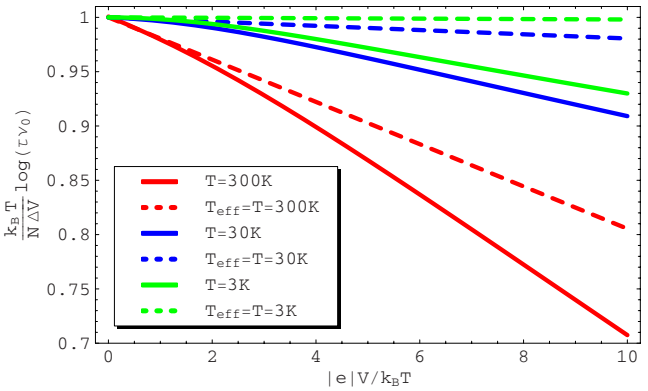

FIG. 7. (Color online) Logarithm of the escape time $(k_BT/N\Delta V)\log\tau\nu_0$ as a function of $|e|V/k_BT$ with (solid curves) and without (dashed curves) current-induced fluctuations. We used $\Delta V\lambda/\xi=1$ meV, $N=10$, $k_F\lambda=1$, $\Delta=\varepsilon_F$, $P=0$, and several temperatures.

IV. DISCUSSION

We have established a microscopic theory that describes the effects of current-induced fluctuations on a domain wall. Since fluctuations in the current influence the system via spin transfer and momentum transfer, we find two separate forces, dampings and effective temperatures that correspond to these processes. We note that the ratio of the momentum transfer and the spin transfer $\beta=F_X/F_\phi$ that we calculate does not yet include the contribution due to spin relaxation. However, this contribution is small compared to the contribution due to momentum transfer when the domain wall is narrow and can therefore be ignored. In addition to the contribution due to the coupling of the domain wall with the electrons in the leads, that we consider here, there is an intrinsic contribution to the damping due to spin relaxation, which is of the order $\alpha_0\sim 0.01-0.1$ in bulk materials, i.e., of the same order as the voltage-dependent damping parameters that we obtain. A voltage-independent contribution to the damping will decrease the effective temperature and thereby increase the depinning time somewhat.

As an application, we have studied depinning of the domain wall from a nanoconstriction. The width of the domain wall in nanocontacts is approximately the same as the nanocontact itself.[17] In experiments, it can be as small as $\lambda\sim 1$ nm,[18,19] which is smaller than the phase coherence length $L_\phi\sim 10$ nm in metals at room temperature and therefore permits a Landauer-Büttiker transport approach. Tatara *et al.*[31] have shown that in nanocontacts in metals Ni and Co, the exchange-splitting energy can reach high values $\Delta/2\varepsilon_F\simeq 0.98$. The voltage on the system in the experiment by Coey *et al.* is of the order $|e|V\sim 0.1$ eV, which leads to $|e|V/k_BT\simeq 4$ at room temperature. The potential barrier in experiments on nanocontacts for typical displacements $\xi\sim 10\lambda$ (Ref. 18) is very large $\Delta V\sim 10$ eV but can be tuned by applying an external magnetic field. We see from Fig. 7 that at room temperature, the current-induced fluctuations already have an effect on depinning times, even if we take into account the fact that polarization might reduce this effect somewhat. At lower temperatures, this effect becomes larger. Under these circumstances, Coey *et al.* find no evidence for heating effects, which would be another source of increased fluctuations. Therefore, current-induced fluctuations should be observable with domain walls in nanocontacts.

Depinning of the angle ϕ is possible for relatively low values of the transverse anisotropy $K_\perp$. This depinning corresponds to switching between Néel walls of different chirality. Between the Néel wall configurations, the domain wall takes the form of a Bloch wall that has higher energy. Coey *et al.*[32] have argued that in nanoconstrictions, the energy difference is comparable to the thermal energy at room temperature. Now, $T_{\mathrm{eff},\phi}$ is the effective temperature of interest and from Fig. 6 we observe that current-induced fluctuations substantially alter this temperature. We therefore expect that effects of current-induced fluctuations on fluctuation-assisted domain-wall transformations can be significant.

ACKNOWLEDGMENTS

This work was supported by the Netherlands Organization for Scientific Research (NWO) and by the European Research Council (ERC) under the Seventh Framework Program. It is a pleasure to thank Henk Stoof for discussions.

APPENDIX: DERIVATION OF THE LANGEVIN EQUATIONS

To find the equations of motion in Eqs. (12) and (13) from the effective action in Eq. (9) we follow the method described in Refs. 21 and 25. The effective action in terms of the coordinates X and ϕ can be written as

$$S_{\text{eff}}[X,\phi] = -\hbar N \int_C dt \left[\frac{X(t)}{\lambda}\dot{\phi}(t) + \frac{K_\perp}{2}\sin 2\phi(t) + F_X\frac{X(t)}{\lambda} + F_\phi\phi(t) \right] - \frac{1}{2}\int\int_C dtdt' \left[\frac{X(t)}{\lambda}\Pi_X(t-t')\frac{X(t')}{\lambda} + \phi(t)\Pi_\phi(t-t')\phi(t') \right]. \tag{A1}$$

We write out the Keldysh contour explicitly using Eq. (11) to find

$$S_{\text{eff}}[X_{\text{cl}},\phi_{\text{cl}},\xi,\kappa] = \hbar N \int_{-\infty}^{+\infty} dt \left\{ \frac{1}{\lambda}[\dot{X}_{\text{cl}}(t)\kappa(t) - \dot{\phi}_{\text{cl}}(t)\xi(t)] - K_\perp \cos 2\phi_{\text{cl}}(t)\sin\kappa(t) - F_X\frac{\xi(t)}{\lambda} - F_\phi\kappa(t) \right\} - \frac{1}{2}\int\int_{-\infty}^{+\infty} dtdt' \left\{ \frac{1}{\lambda^2}\left[X_{\text{cl}}(t)\Pi_X^{(-)}(t-t')\xi(t') + \xi(t)\Pi_X^{(+)}(t-t')X_{\text{cl}}(t') + \frac{1}{2}\xi(t)\Pi_X^{\text{K}}(t-t')\xi(t') \right] + \phi_{\text{cl}}(t)\Pi_\phi^{(-)}(t-t')\kappa(t') + \kappa(t)\Pi_\phi^{(+)}(t-t')\phi_{\text{cl}}(t') + \frac{1}{2}\kappa(t)\Pi_\phi^{\text{K}}(t-t')\kappa(t') \right\}. \tag{A2}$$

The response functions that are introduced in Eqs. (16) and (17) are the Fourier transforms of the functions $\Pi_i^{(\pm)}(t-t')$ and $\Pi_i^{\text{K}}(t-t')$ that appear in the above expression. We perform two Hubbard-Stratonovich transformations to decouple the terms quadratic in ξ and κ to find that the probability distribution is given by

$$\begin{aligned} P \propto & \int d[X_{\text{cl}}]\int d[\phi_{\text{cl}}]\int d[\xi]\int d[\kappa] e^{i/\hbar S_{\text{eff}}[X_{\text{cl}},\phi_{\text{cl}},\xi,\kappa]} \\ & \times \int d[\eta_X] e^{i/4\hbar\lambda^2 \int\int dtdt'[\xi(t)+2\hbar N\lambda\int dt''\eta_X(t'')(\Pi_X^{\text{K}})^{-1}(t''-t)]\Pi_X^{\text{K}}(t-t')[\xi(t')+2\hbar N\lambda\int dt'''(\Pi_X^{\text{K}})^{-1}(t'-t''')\eta_X(t''')]} \\ & \times \int d[\eta_\phi] e^{i/4\hbar\int\int dtdt'[\kappa(t)-2\hbar N\int dt''\eta_\phi(t'')(\Pi_\phi^{\text{K}})^{-1}(t''-t)]\Pi_\phi^{\text{K}}(t-t')[\kappa(t')-2\hbar N\int dt'''(\Pi_\phi^{\text{K}})^{-1}(t'-t''')\eta_\phi(t''')]} \\ \propto & \int d[X_{\text{cl}}]\int d[\phi_{\text{cl}}]\int d[\xi]\int d[\kappa]\int d[\eta_X]\int d[\eta_\phi] e^{i\hbar N^2\int\int dtdt'[\eta_X(t)(\Pi_X^{\text{K}})^{-1}(t-t')\eta_X(t')+\eta_\phi(t)(\Pi_\phi^{\text{K}})^{-1}(t-t')\eta_\phi(t')]} \\ & \times e^{-iN\int dt\{\dot{\phi}_{\text{cl}}(t)+1/2\hbar N\int dt' X_{\text{cl}}(t')/\lambda[\Pi_X^{(+)}(t-t')+\Pi_X^{(-)}(t'-t)]+F_X-\eta_X(t)\}\xi(t)/\lambda} \\ & \times e^{iN\int dt\{\dot{X}_{\text{cl}}(t)/\lambda-1/2\hbar N\int dt'\phi_{\text{cl}}(t')[\Pi_\phi^{(+)}(t-t')+\Pi_\phi^{(-)}(t'-t)]-K_\perp\cos 2\phi_{\text{cl}}(t)-F_\phi-\eta_\phi(t)\}\kappa(t)}, \end{aligned} \tag{A3}$$

where η_X and η_ϕ are introduced by the Hubbard-Stratonovich transformations. Note that the sign of these stochastic contributions is not important. (Note that we used that κ is small to write $\sin\kappa \simeq \kappa$.) Carrying out the functional integral over $\xi(t)$ and $\kappa(t)$ leads to delta functionals that constrain ϕ_{cl} and X_{cl}. These constraints are precisely the desired equations of motion, given by

$$\frac{\dot{X}_{\text{cl}}(t)}{\lambda} - \frac{1}{2\hbar N}\int dt'\,\phi_{\text{cl}}(t')[\Pi_\phi^{(+)}(t-t') + \Pi_\phi^{(-)}(t'-t)] = K_\perp\cos 2\phi_{\text{cl}}(t) + F_\phi + \eta_\phi(t), \tag{A4}$$

$$\dot{\phi}_{\rm cl}(t) + \frac{1}{2\hbar N}\int dt' \frac{X_{\rm cl}(t')}{\lambda}[\Pi_X^{(+)}(t-t') + \Pi_X^{(-)}(t'-t)] = -F_X + \eta_X(t). \quad \text{(A5)}$$

We arrive at Eqs. (12) and (13) by using that in the low-frequency limit

$$\int dt' \Pi_X^{(+)}(t-t')X_{\rm cl}(t') = \int dt' X_{\rm cl}(t')\Pi_X^{(-)}(t'-t) = \hbar N \alpha_X \dot{X}_{\rm cl}(t), \quad \text{(A6)}$$

and similar for $\phi_{\rm cl}$. From the fourth line of Eq. (A3) we read off that the variance of the stochastic forces is given by $\langle \eta_i(t)\,\eta_i(t')\rangle \propto \Pi_i^{\rm K}(t-t')$.

*m.e.lucassen@uu.nl

[1] A. Einstein, Ann. Phys. (Leipzig) **322**, 549 (1905).
[2] M. J. M. de Jong and C. W. J. Beenakker, in *Mesoscopic Electron Transport*, Vol. 345 of NATO Advanced Studies Institute, Series E: Applied Science , edited by L. L. Sohn, L. P. Kouwenhoven, and G. Schoen (Kluwer Academic, Dordrecht, 1997).
[3] L. Berger, J. Appl. Phys. **55**, 1954 (1984).
[4] P. P. Freitas and L. Berger, J. Appl. Phys. **57**, 1266 (1985).
[5] J. C. Slonczewski, J. Magn. Magn. Mater. **159**, L1 (1996).
[6] L. Berger, Phys. Rev. B **54**, 9353 (1996).
[7] G. Tatara and H. Kohno, Phys. Rev. Lett. **92**, 086601 (2004); **96**, 189702 (2006).
[8] J. Grollier, P. Boulenc, V. Cros, A. Hamzić, A. Vaurès, and A. Fert, Appl. Phys. Lett. **83**, 509 (2003).
[9] M. Kläui, C. A. F. Vaz, J. A. C. Bland, W. Wernsdorfer, G. Faini, and E. Cambril, Appl. Phys. Lett. **83**, 105 (2003).
[10] A. Yamaguchi, T. Ono, S. Nasu, K. Miyake, K. Mibu, and T. Shinjo, Phys. Rev. Lett. **92**, 077205 (2004).
[11] G. S. D. Beach, C. Nistor, C. Knutson, M. Tsoi, and J. L. Erskine, Nature Mater. **4**, 741 (2005).
[12] M. Yamanouchi, D. Chiba, F. Matsukura, T. Dietl, and H. Ohno, Phys. Rev. Lett. **96**, 096601 (2006).
[13] S. Zhang and Z. Li, Phys. Rev. Lett. **93**, 127204 (2004).
[14] M. Hayashi, L. Thomas, C. Rettner, R. Moriya, Y. B. Bazaliy, and S. S. P. Parkin, Phys. Rev. Lett. **98**, 037204 (2007).
[15] L. Heyne, M. Klaüi, D. Backes, T. A. Moore, S. Krzyk, U. Rüdiger, L. J. Heyderman, A. F. Rodríguez, F. Nolting, T. O. Mentes, M. Á. Niño, A. Locatelli, K. Kirsch, and R. Mattheis, Phys. Rev. Lett. **100**, 066603 (2008).
[16] M. Feigenson, J. W. Reiner, and L. Klein, Phys. Rev. Lett. **98**, 247204 (2007).
[17] P. Bruno, Phys. Rev. Lett. **83**, 2425 (1999).
[18] J. J. Versluijs, M. A. Bari, and J. M. D. Coey, Phys. Rev. Lett. **87**, 026601 (2001).
[19] N. García, M. Muñoz, and Y.-W. Zhao, Phys. Rev. Lett. **82**, 2923 (1999).
[20] J. Foros, A. Brataas, Y. Tserkovnyak, and G. E. W. Bauer, Phys. Rev. Lett. **95**, 016601 (2005).
[21] A. S. Núñez and R. A. Duine, Phys. Rev. B **77**, 054401 (2008).
[22] A. L. Chudnovskiy, J. Swiebodzinski, and A. Kamenev, Phys. Rev. Lett. **101**, 066601 (2008).
[23] J. Foros, A. Brataas, Y. Tserkovnyak, and G. E. W. Bauer, Phys. Rev. B **78**, 140402 (2008).
[24] D. M. Basko and M. G. Vavilov, Phys. Rev. B **79**, 064418 (2009).
[25] H. T. C. Stoof, J. Low Temp. Phys. **114**, 11 (1999).
[26] R. A. Duine, A. S. Núñez, and A. H. MacDonald, Phys. Rev. Lett. **98**, 056605 (2007).
[27] A. Mitra and A. J. Millis, Phys. Rev. B **72**, 121102(R) (2005).
[28] I. I. Mazin, Phys. Rev. Lett. **83**, 1427 (1999).
[29] X. Waintal and M. Viret, Europhys. Lett. **65**, 427 (2004).
[30] H. Katsura, A. V. Balatsky, Z. Nussinov, and N. Nagaosa, Phys. Rev. B **73**, 212501 (2006).
[31] G. Tatara, Y.-W. Zhao, M. Muñoz, and N. García, Phys. Rev. Lett. **83**, 2030 (1999).
[32] J. M. D. Coey, L. Berger, and Y. Labaye, Phys. Rev. B **64**, 020407(R) (2001).